

Crystallization of a coprecipitated mullite precursor during heat treatment

S. RAJENDRAN, H. J. ROSSELL, J. V. SANDERS

CSIRO, Division of Materials Science and Technology, Locked Bag 33, Clayton, Victoria 3168, Australia

Powder of mullite composition ($3\text{Al}_2\text{O}_3 \cdot 2\text{SiO}_2$) has been made by a coprecipitation method. The evolution of mullite in this precursor powder during heat treatment has been studied using differential thermal analysis, electron microscopy and X-ray diffraction techniques. It is shown that during calcination below 1100°C the coprecipitate develops $\gamma\text{-Al}_2\text{O}_3$ and perhaps cristobalite crystallites within the basic grains, whose morphology is otherwise invariant with temperature. Mullite forms above 1100°C by reaction of these $\gamma\text{-Al}_2\text{O}_3$ and SiO_2 crystallites, and the grain morphology changes markedly. Small exothermic events occur at 1000 and 1250°C . The former is associated with the decomposition of a small content of aluminosilicate or perhaps with the conversion of γ - to $\theta\text{-Al}_2\text{O}_3$, and the latter with mullite formation. For comparison, the behaviour of a polymeric mullite precursor during calcination is also examined. This material showed a large exothermic event at 1000°C which could be associated with the decomposition of the (amorphous) aluminosilicate to crystalline $\gamma\text{-Al}_2\text{O}_3$ and SiO_2 , and a small exothermic event at 1250°C due to mullite formation.

1. Introduction

Mullite is the only stable crystalline compound in the $\text{Al}_2\text{O}_3\text{-SiO}_2$ system at atmospheric pressure [1]; its composition varies from $3\text{Al}_2\text{O}_3 \cdot 2\text{SiO}_2$ to $2\text{Al}_2\text{O}_3 \cdot \text{SiO}_2$. This material is of technological importance because of its moderate thermal expansion [2] and high creep resistance [3]. Mullite is made usually by the reaction of mixed alumina and silica powders or mineral precursors at 1600 to 1700°C for several hours. The product commonly has variable composition so that sintered bodies contain an excess of alumina or silica as a second phase [1].

Attempts have been made to produce mullite of more uniform composition and at lower temperatures from powders prepared via chemical routes such as coprecipitation or sol-gel procedures [4-15]. There have been several studies of the thermal behaviour of such precursor powders during calcination. In some cases, two exothermic events, one at 980 to 1000°C and the other at about 1250°C , have been observed in differential thermal analysis (DTA) work [13, 15, 16]. Such results have been explained in several ways, including the crystallization of Si-Al spinel at about 1000°C and its transformation to mullite at the higher temperature. On the other hand, there have been instances where only one or the other of these exothermic events has been observed, with reports that the events at either temperature were due to the formation of mullite [11, 14].

There seems to have been no detailed examination of the evolution of mullite from chemically produced precursor powders. This paper reports some results from transmission electron microscopy and powder

X-ray diffraction applied to powders of mullite composition that were prepared by a coprecipitation procedure and calcined in the range 20 to 1700°C .

2. Experimental procedure

Aluminium-silicon hydrated oxide containing 60 mol % Al_2O_3 and 40 mol % SiO_2 was prepared by coprecipitation. Required proportions of stock solutions of AR aluminium nitrate in water (~ 2 M) and of tetramethoxy orthosilicate in methanol (~ 0.15 ml/ml methanol) were mixed and added to continuously stirred AR ammonia solution. The precipitation was carried out in an atmosphere of nitrogen. The pH was adjusted finally to 9.0 , and the stirring continued for 1 h. The product was kept at room temperature for $1/2$ h, filtered and washed with deionized water until free from nitrate, dispersed ultrasonically in acetone twice, then dried in a vacuum oven at 75°C for 24 h.

Differential thermal analyses and thermogravimetric analyses (TGA) of this material were done simultaneously using a Stanton-Redcroft derivatograph operated from 20 to 1400°C at a heating rate of $10^\circ\text{C min}^{-1}$ and using 40 mg samples.

X-ray diffraction (XRD) and transmission electron microscopical (TEM) analyses were carried out on samples of the oven-dried coprecipitate that had been heated in air at several selected temperatures for 2 h.

Powder XRD patterns were recorded with a Rigaku diffractometer using filtered $\text{CuK}\alpha$ radiation and scanning rate of 2°C min^{-1} . Powder XRD photographs were taken with a Guinier-Lenné focusing camera. This device operates with $\text{CuK}\alpha_1$ radiation, and can produce on steadily moving film a continuous

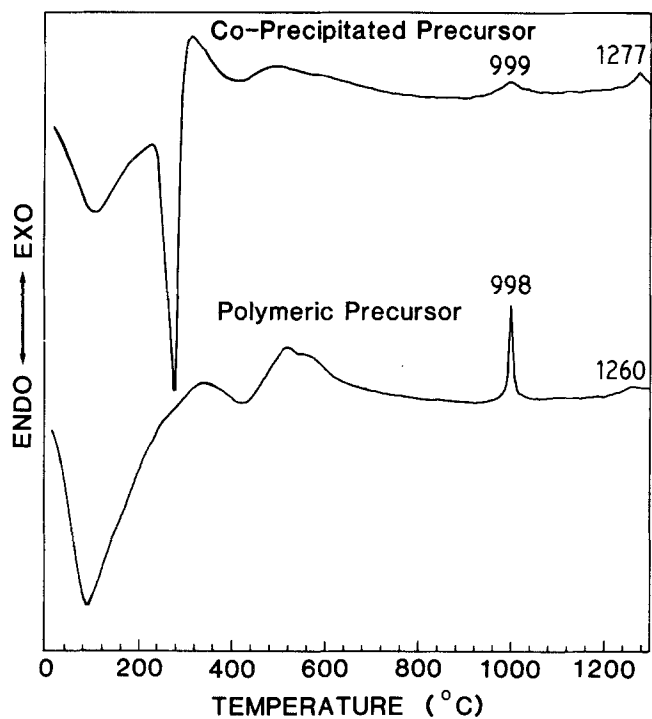


Figure 1 DTA curves of oven-dried (a) coprecipitated and (b) polymeric precursor powders.

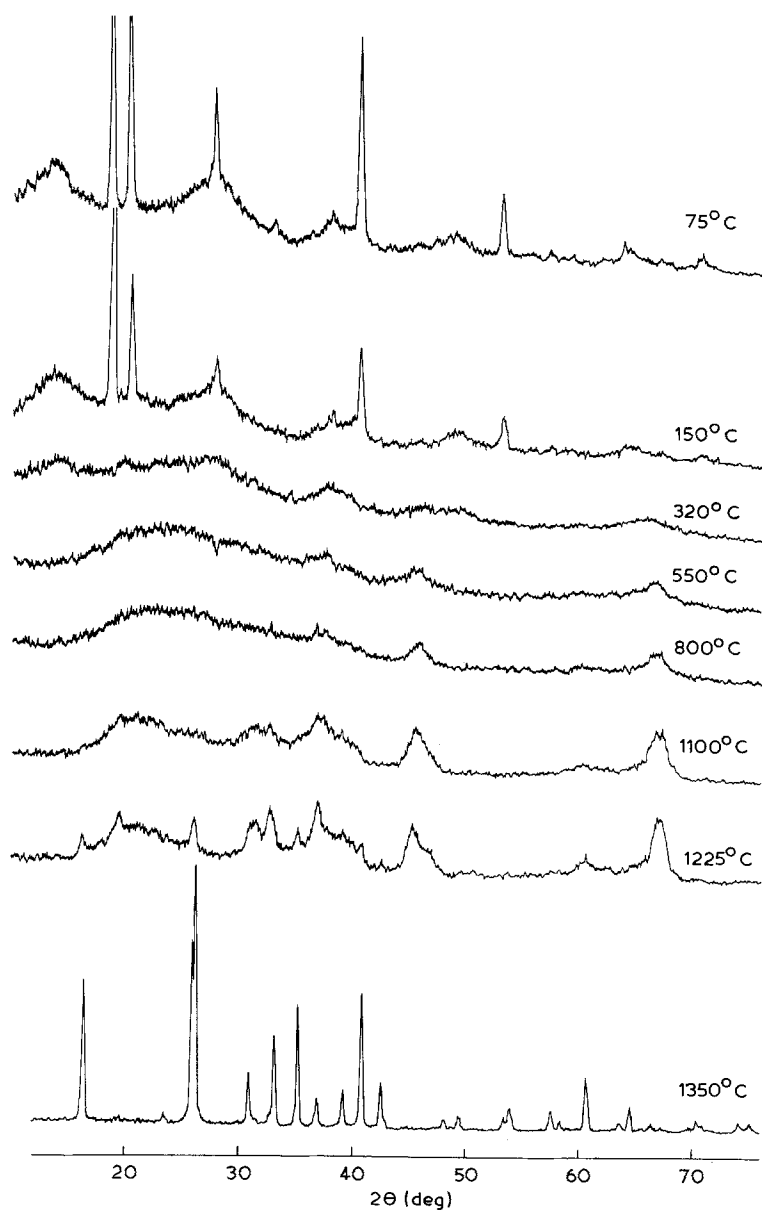


Figure 2 Room-temperature XRD (diffractometer) patterns of coprecipitated material calcined at different temperatures.

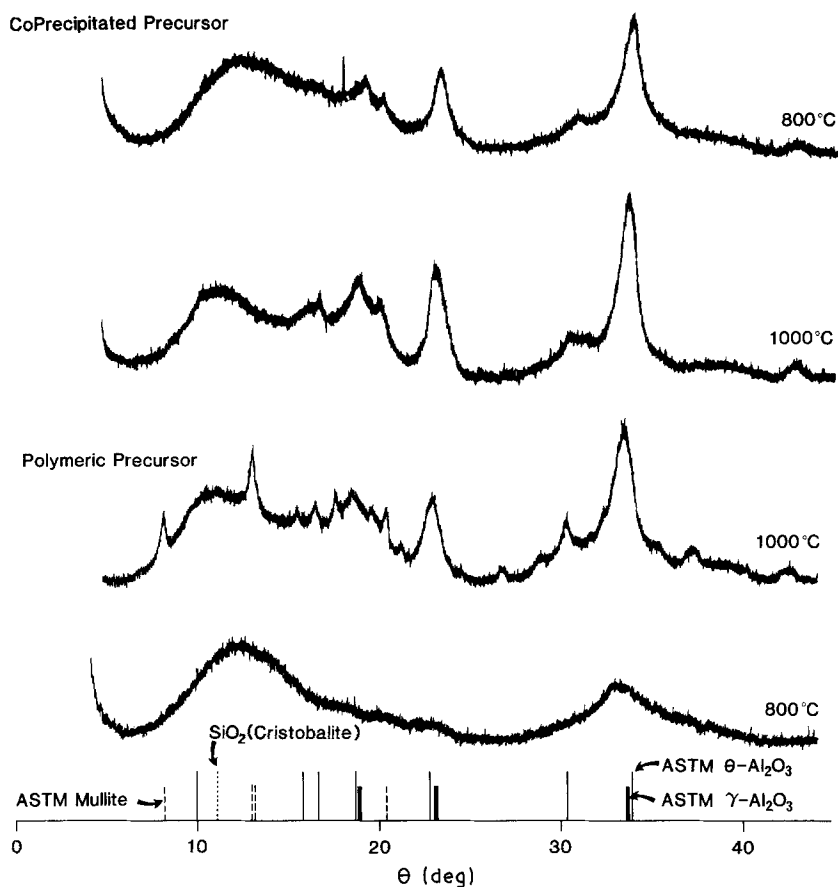


Figure 3 Guinier XRD patterns of specimens of (a) coprecipitated and (b) polymeric precursors heated for 20 min at 800 and 1000°C.

photographic record of the diffraction pattern as the specimen is heat-treated according to a desired programme in the range 20 to 1500°C. Linear heating rates of 50°C h⁻¹ and film speeds of 1 mm h⁻¹ were usually necessary for satisfactory exposures.

Specimens for TEM were prepared by evaporation of an ethanolic dispersion of the powder on grids coated with perforated carbon film. They were examined in a Jeol 100CX electron microscope (top entry, $C_s = 0.7$ mm). Because it was often necessary to detect diffuse electron diffraction effects from poorly crystalline material, care was taken to obtain diffraction patterns from fragments of the specimens suspended over holes in the carbon film to avoid the superposition of diffuse scattering from the carbon.

A mullite precursor was also made by controlled hydrolysis of mixed tetraethylorthosilicate and aluminium isopropoxide under conditions expected to produce a polymeric aluminosiloxane product [16], and oven-dried. The chemical constitution of such a precursor is different to that of the above coprecipitated precursor, and it was of interest to compare the behaviour of each during calcination.

3. Results

3.1. Thermal analysis

DTA results from the oven-dried coprecipitated powder are given in Fig. 1. The DTA curve shows three endothermic peaks at 110, 290 and 420°C and two small exothermic peaks near 1000 and 1280°C. All three endothermic peaks are associated with weight losses, the sum of which is 31%. DTA results from the oven-dried polymeric precursor also are shown in the figure, and it can be seen that the exotherm near

1000°C is much more pronounced in this case.

3.2. Powder X-ray diffraction

X-ray diffractograms of the oven-dried coprecipitated samples that had been calcined for 2 h at various temperatures are given in Fig. 2. Samples calcined at 75 and 150°C consisted of at least two phases, a well-crystallized bayerite ($\text{Al}(\text{OH})_3$) and an amorphous phase. For powder calcined at 320°C, the diffraction peaks of bayerite had disappeared, and the whole specimen appeared amorphous to X-rays. Specimens calcined at higher temperatures (550 to 1100°C) also were amorphous or cryptocrystalline. However, the crystallinity of the samples gradually improved with increase of calcination temperature. Material calcined at 1100°C gave diffraction peaks due to $\gamma\text{-Al}_2\text{O}_3$, while peaks due to $\gamma\text{-Al}_2\text{O}_3$ and mullite occurred in patterns of materials heated to 1225°C. Specimens calcined at 1350°C gave only the peaks expected for mullite of composition $3\text{Al}_2\text{O}_3 \cdot 2\text{SiO}_2$.

The X-ray powder diffraction photographs taken with the Guinier-Lenné camera gave results in accord with those above. The only detectable crystalline phase present in uncalcined coprecipitated material was bayerite; this persisted on heating to 230°C, when it disappeared abruptly. The background intensity rose sharply at this temperature, indicating that the specimen had become amorphous to X-rays. No crystalline phase was apparent on further heating until approximately 1000°C, when very diffuse diffraction lines due to very small crystallites of $\gamma\text{-Al}_2\text{O}_3$ appeared. These lines increased in intensity and sharpened as the temperature increased beyond

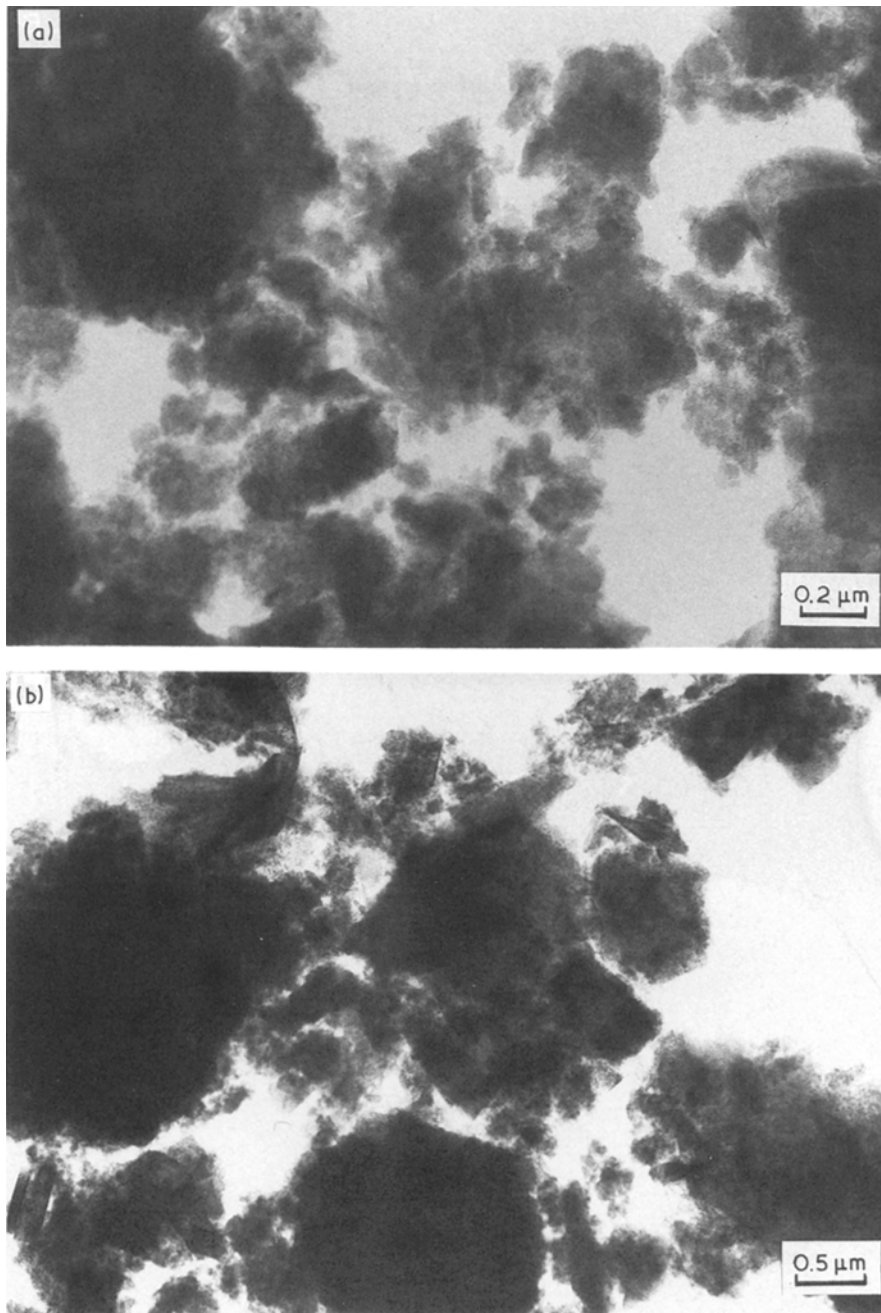


Figure 4 Transmission electron micrographs of fragments of the coprecipitated powders after heating at (a) 75°C and (b) 1100°C.

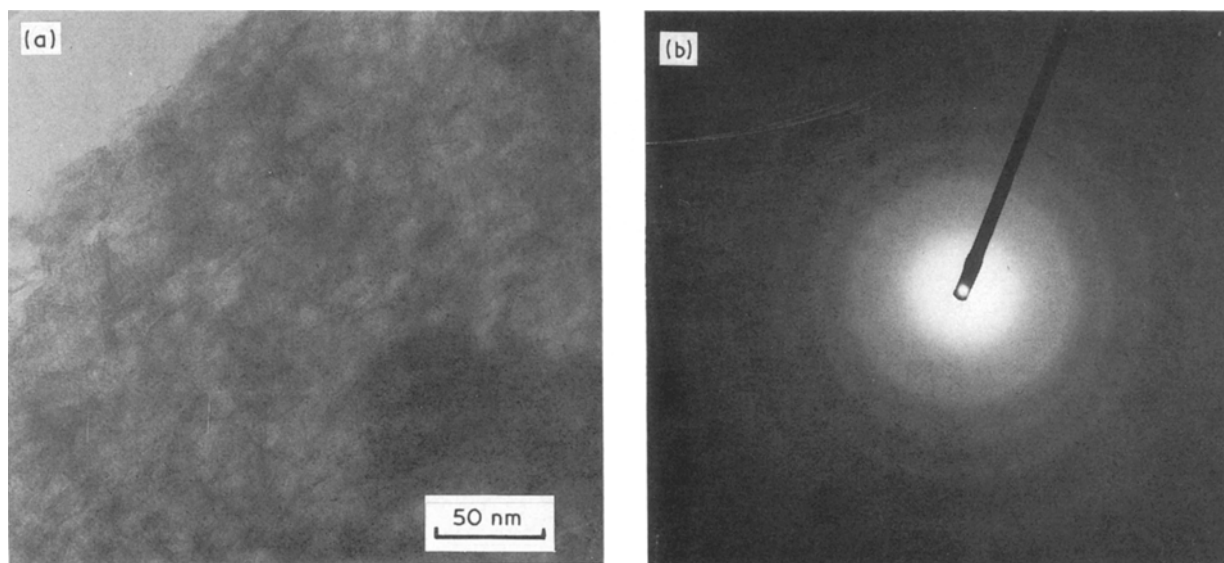


Figure 5 Transmission electron micrograph (a), and electron diffraction pattern (b) of the thin edge of a fragment of coprecipitated powder after calcination at 75°C. Many fragments gave even more diffuse patterns, and frequently no rings or haloes could be seen.

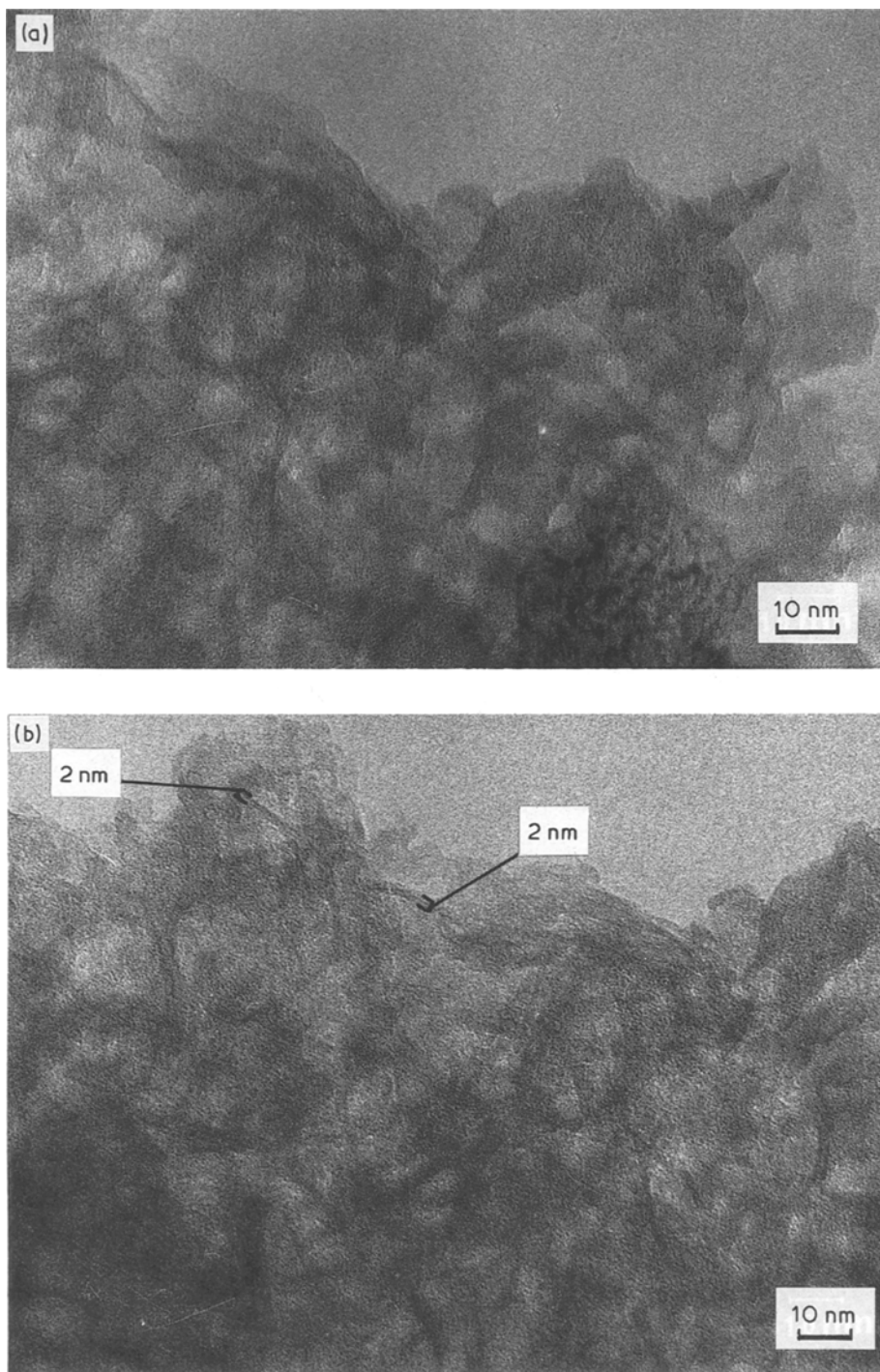


Figure 6 Transmission electron micrographs of edges of fragments, calcined at 75° C at high magnification. It is believed that the fragments consist of an agglomerate of plates about 2 nm thick: these are seen normally in (a) and parallel in (b).

1000° C, indicating growth of the γ -Al₂O₃ crystallites to 10 to 20 nm diameter; this size estimate was approximate only, because of the weakness of the lines. The γ -Al₂O₃ persisted in this form until 1190° C, when sharp diffraction lines due to mullite appeared. The latter increased rapidly in intensity at the expense of the γ -Al₂O₃ lines and the enhanced background as the temperature increased: by 1250° C, the only crystalline phase present was mullite. This phase was retained on further heating to 1400° C, and during subsequent cooling to room temperature.

Fig. 3 shows Guinier XRD patterns, taken at room temperature, of specimens of coprecipitated and of polymeric precursors that had been heated for 20 min

at 800° C, and of the same specimens further heated at 1000° C for 20 min, i.e. the temperature at which an exothermic event occurred. The temperatures and times were chosen as a reasonable approximation to the conditions experienced by a specimen in the DTA device. No supporting material was used for the specimen so as to preclude the production of any spurious peaks. After heating at 800° C the coprecipitated material displayed broad diffraction peaks due to very small crystallites of γ -Al₂O₃ and a very broad peak near $d = 0.37$ nm which is not part of the expected γ -Al₂O₃ pattern, and which must be ascribed to the SiO₂ present in the specimen. On heating further at 1000° C, the only changes in the XRD pattern apart

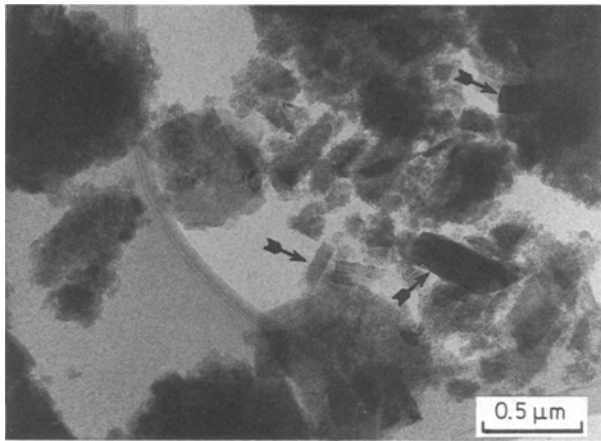


Figure 7 Coprecipitated powder heated at 150°C for 2 h contained a small concentration of rectangular crystals (arrowed), which were identified by electron diffraction as aluminium hydroxide in various states of hydration.

from a slight sharpening of the peaks due to crystallite growth, were that some extra broad peaks due to θ - Al_2O_3 appeared, and the broad peak at $d = 0.37$ nm had sharpened and shifted to $d = 0.405$ nm, so that it could be confidently associated with small cristobalite (SiO_2) crystallites. It was not possible to estimate crystallite sizes from these patterns, because most peaks contained two or more overlapping reflections.

By comparison, the XRD pattern for the polymeric precursor after heating at 800°C was largely featureless, and corresponded to that expected for nearly amorphous aluminosilicate material (ASTM Index of Powder Patterns), but after heating for 20 min at 1000°C, the specimen had changed considerably, and the XRD pattern showed broad peaks due to major amounts of small γ - Al_2O_3 and cristobalite crystallites, together with a smaller amount of mullite, also of small crystallite size.

3.3. Electron microscopy

TEM analysis of the coprecipitated samples calcined at 75 and 150°C indicated the presence of three components. The major component consisted of porous fragments of irregular shape, 0.1 to 2 μm in size (Fig. 4a). Each fragment was made up of plates of irregular shape and size, approximately 10 nm wide and 1 to 2 nm thick (Figs 5 and 6). Electron diffraction patterns from such fragments contained very diffuse, hardly detectable haloes, or a set of weak diffuse rings with spacings consistent with those from $\text{Al}(\text{OH})_3$ (Fig. 5b).

Fragments as above occasionally contained embedded small crystals, which were irregular in shape and about 0.1 μm in size (Fig. 7). Their presence was shown by spots in the diffraction patterns, and their distribution could be seen in dark-field images formed from beams corresponding to such spots. There was insufficient information in the electron diffraction patterns to identify this phase positively.

The third component was of rare occurrence, and consisted of rectangular crystals about 1 μm in size, which could be selected and tilted in the electron microscope to give zone axis diffraction patterns. These enabled identification of the crystals to be made. Both the gibbsite and bayerite forms of $\text{Al}(\text{OH})_3$ were found in specimens dried at 75°C, but only bayerite was identified in specimens heated to 150°C.

Specimens heated at 320°C contained mostly an amorphous, spongy phase that gave a very diffuse electron diffraction pattern. There was a very small concentration of very poorly crystallized γ - Al_2O_3 .

The morphology of the specimens was unchanged with increasing calcination temperature, and the fragments appeared similar to those in the oven-dried (75°C) specimens (Fig. 4b). However, the crystallinity of the specimens improved with increasing calcination temperature.

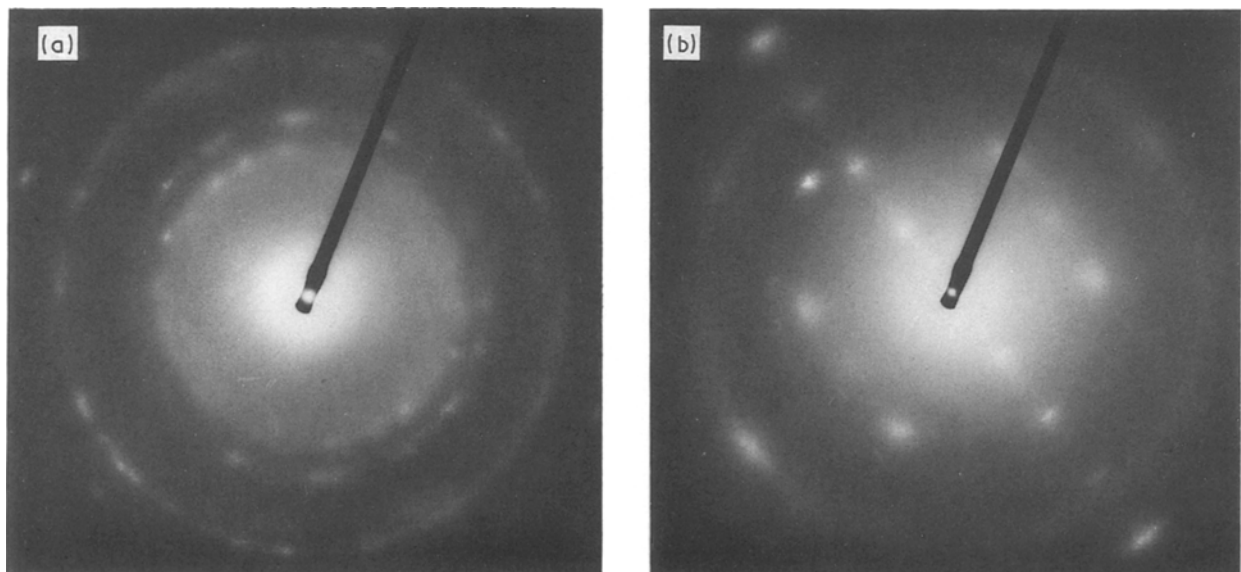


Figure 8 Coprecipitated powder heated at 800°C. Partial crystallization to γ - Al_2O_3 has occurred. Electron diffraction patterns are diffuse, and most fragments give ring patterns from a polycrystalline aggregate (a). However some fragments contain extensive areas of local order (b), and hence give a net of spots. The diffuse nature of the spots indicates extensive disorder in the crystal, or that it is an assembly of small volumes of order in the same orientation.

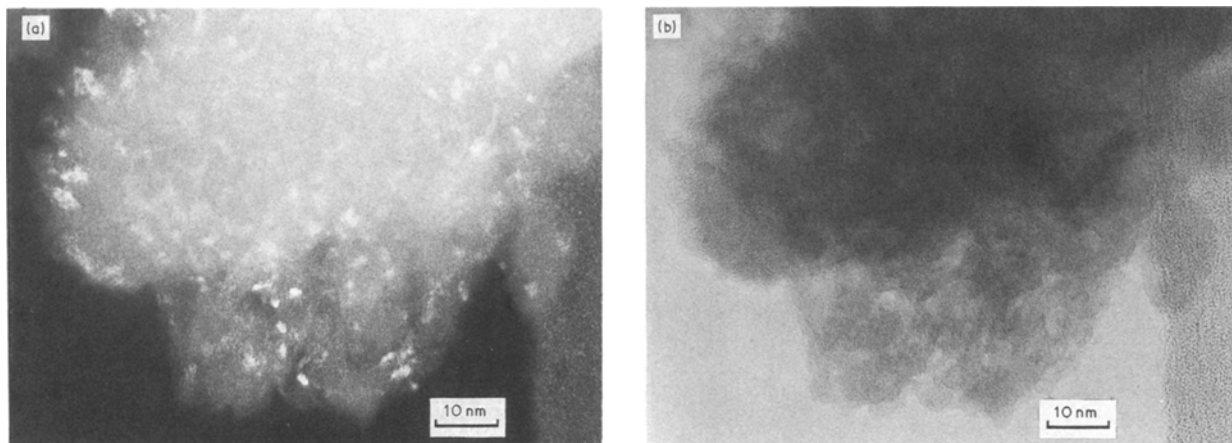


Figure 9 (a) Dark-field image of material after heat treatment at 800°C. The size and distribution of the γ -Al₂O₃ crystals within a fragment can be seen, as bright areas (5 to 10 nm) scattered uniformly throughout the fragment. Only part of the crystalline content can be shown in such a single electron micrograph. The crystals cannot be recognized in the bright-field image (b).

The electron diffraction pattern of the major component in specimens calcined at 800°C consisted of diffuse rings and very diffuse spots (Fig. 8). The rings corresponded to the more intense reflections of γ -Al₂O₃ (3 1 1, 4 0 0, 4 4 0), and the spots similarly were due to γ -Al₂O₃. Dark-field images (Fig. 9) indicated that each fragment was polycrystalline with a grain size of 1 to 5 nm. High-resolution images showed no regular structure within these grains. No electron diffraction evidence for the presence of silica could be discerned.

The morphology of the fragments was unchanged even in specimens calcined at 1100°C (Fig. 4b). However, the crystallinity had improved, as shown by a sharpening of the rings in the electron diffraction patterns, and the occurrence of diffraction spots in nets (Figs 10 and 11a). The latter came from fragments of about 0.5 μ m diameter, and were indicative of crystalline ordering over a complete fragment in some cases. Most fragments were polycrystalline, and gave electron diffraction patterns consistent with

those expected for γ -Al₂O₃. In one pattern, in addition to the rings from γ -Al₂O₃, there was a diffuse halo corresponding to a spacing of about 0.41 nm, as expected from amorphous SiO₂ (arrowed in Fig. 10b). In other patterns, there was no evidence of such a halo.

High-magnification phase-contrast images of specimens calcined at 1100°C now contained low contrast but clear sets in fringes which could not be detected in specimens calcined at lower temperatures. No sintering had occurred after this heat treatment: however, the individual plates were better ordered crystallographically, and in some fragments the ordering was so extensive that they were effectively single crystals.

The morphology of the fragments was completely changed after heat treatment at 1350°C. The sample appeared homogeneous, and consisted of polycrystalline fragments of about the same overall size as before, but with a grain size of about 0.1 μ m (Fig. 12).

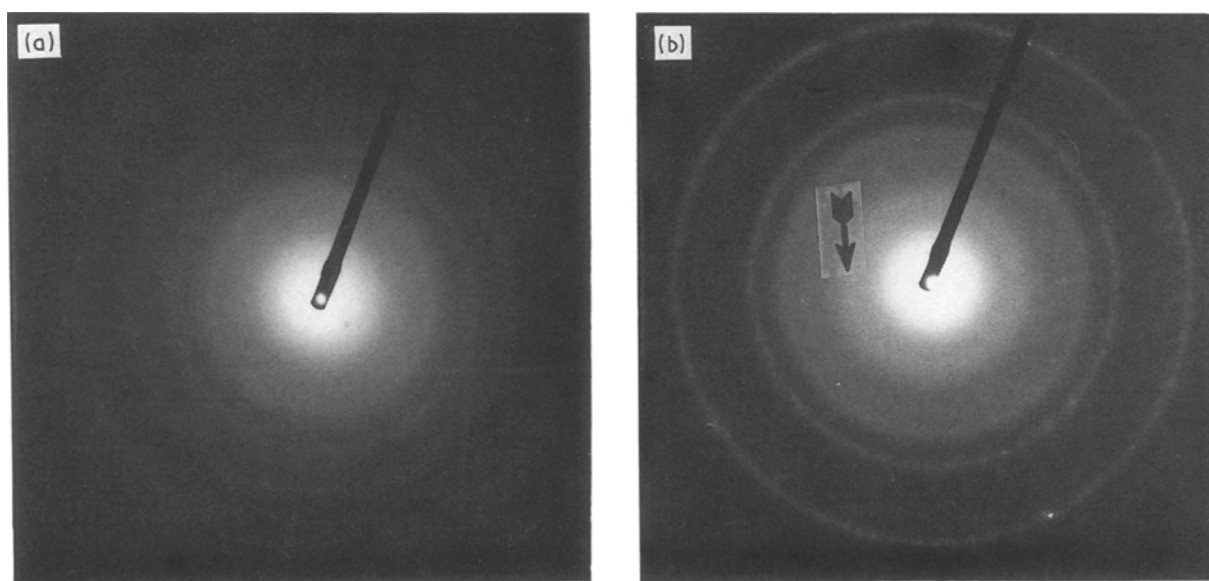


Figure 10 Electron diffraction patterns from typical fragments of coprecipitate after heat treatment at (a) 75°C, (Bayerite, Al(OH)₃), (b) 1100°C, (γ -Al₂O₃). The rings in (b) are sharper than in those in Fig. 8, indicating an increase in perfection of crystallization or some crystal growth. The arrow in (b) points to the halo, whose position corresponds to a spacing of about 0.41 nm, which is expected for amorphous silica. There is no similar halo in the pattern in (a), nor was one observed on any other occasion.

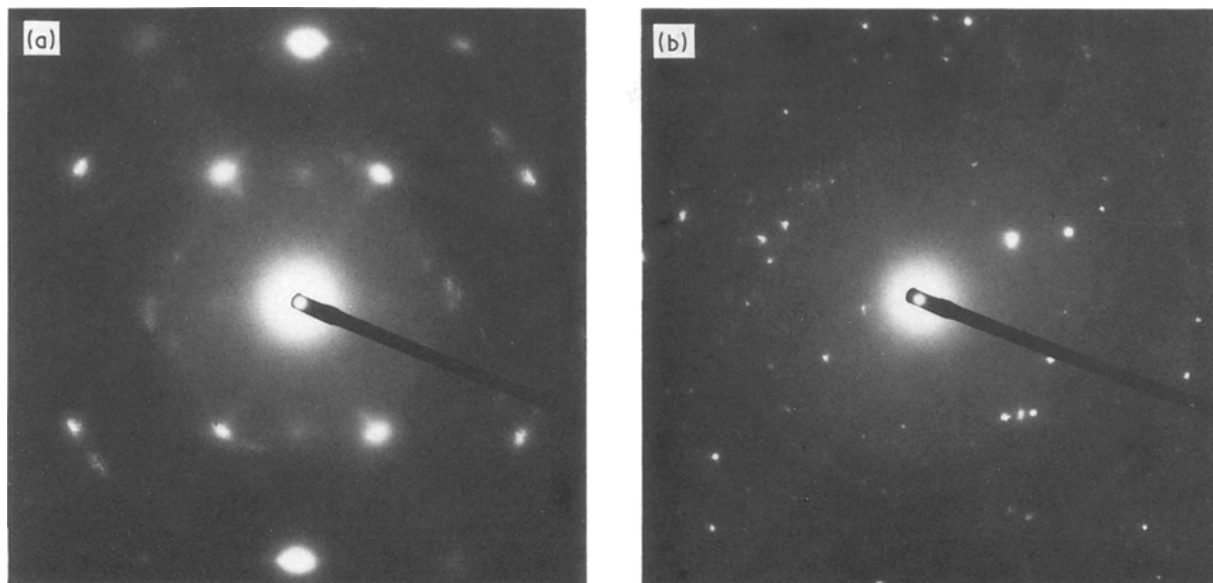


Figure 11 Electron diffraction patterns after heat treatment at (a) 1100°C and (b) 1350°C. The diffuse spots from γ -Al₂O₃ are replaced by sharp spots in with spacings appropriate to mullite.

The corresponding electron diffraction patterns contained sharp spots, and were consistent with those expected for mullite (Fig. 11b). Thus the material had sintered and recrystallized to become homogeneous, fine-grained mullite.

Some representative scanning electron micrographs of pressed specimens that had been sintered conventionally in air at 1600, 1650 and 1700°C for 2 h are shown in Fig. 13. The rapid development of coarse-grained mullite under these conditions is apparent.

4. Discussion

The coprecipitated material, after drying at 75°C consists mainly of amorphous or nearly amorphous fragments of aluminium hydroxide, within which is embedded small crystals of perhaps α - or β -AlOOH, with a small concentration of separate rectangular crystals of bayerite and gibbsite. These details only could be discerned using the sensitive technique of electron diffraction. X-rays are diffracted less strongly than electrons, so that only the bayerite could be detected in XRD: despite its low concentration, its crystals were relatively large and well developed.

The first DTA endotherm at 110°C can be

explained as due to the removal of loosely bound or physisorbed water, probably from the relatively large proportion of the sample demonstrated to be amorphous. From the TEM and XRD results, and noting the relative values of the corresponding weight losses, it can be inferred that the endotherms at 290 and 420°C are associated with the removal of chemically-bound water, e.g. as in the dehydration of bayerite.

The morphology of the powder remains unchanged with heating at least up to 1100°C, but crystallization to γ -Al₂O₃ commences at about 800°C, and is further developed by 1100°C. At 1190 to 1250°C, fine-grained polycrystalline mullite of different morphology forms by reaction of the Al₂O₃ with silica.

Silica undoubtedly was present at all times in the specimens. The XRD evidence suggests that it was present as very small (< 10 nm) crystallites of SiO₂ at 800°C, and of cristobalite at 1000°C. In general, silica was not detected either by electron diffraction (except in one instance where there was diffraction evidence for amorphous silica), or by high-resolution TEM images. Therefore, it was not possible to determine positively the nature, form or distribution of silica in the pre-mullite material.

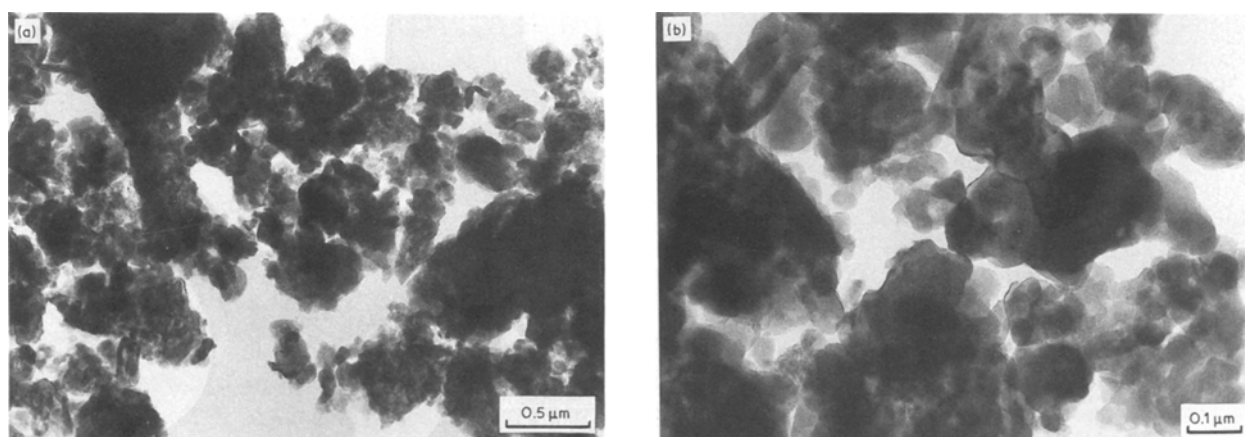


Figure 12 Transmission electron micrographs of a sample after heat treatment at 1350°C. The fragments are now coarse-grained mullite.

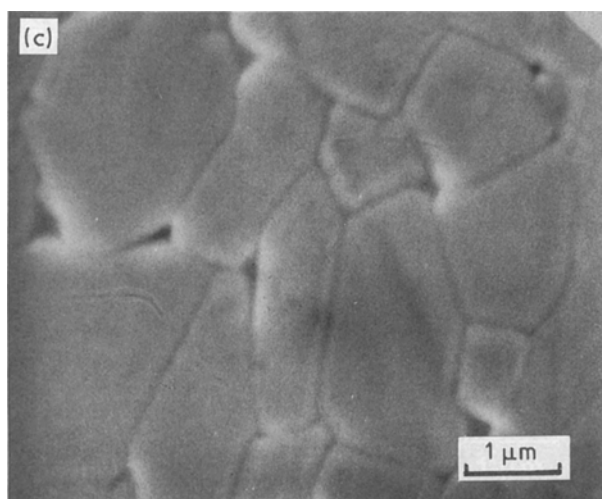
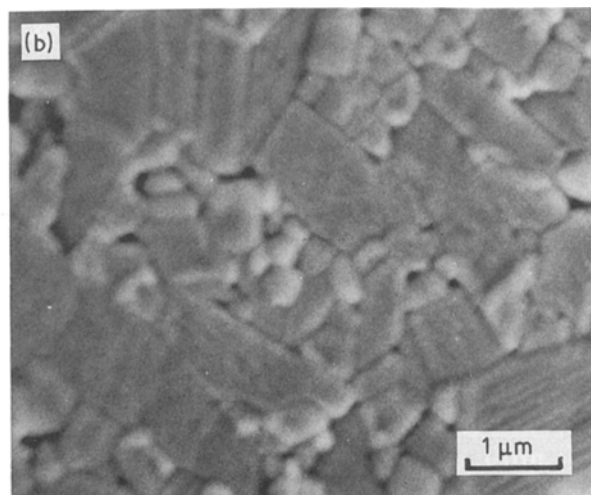
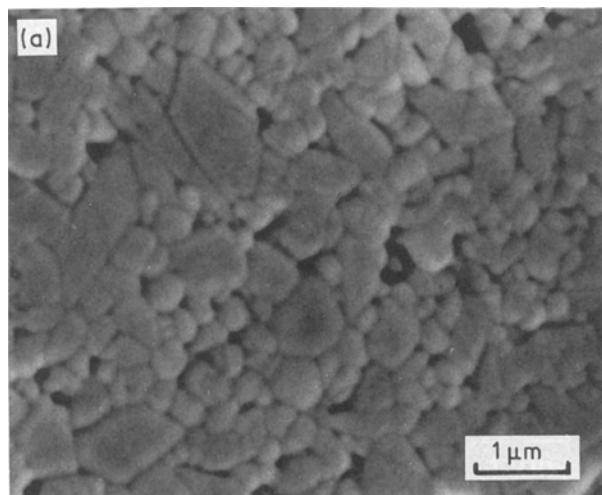


Figure 13 Scanning electron micrographs of mullite ($3\text{Al}_2\text{O}_3 \cdot 2\text{SiO}_2$) from coprecipitate sintered at (a) 1600, (b) 1650 and (c) 1700°C for 2 h.

The exothermic events shown in the DTA records at about 1000 and 1280°C are characteristic of aluminosilicate materials. Thus aluminosilicate clay minerals all exhibit such exothermic DTA peaks [17, 18], as do mullite precursors prepared as polymeric aluminosiloxanes. It is generally agreed that for mullite precursors the exothermic event near 1000°C is due to the crystallization of $\gamma\text{-Al}_2\text{O}_3$ (spinel) [19]. The composition of this spinel when formed from aluminosilicate materials has been the subject of controversy. Evidence has been presented to suggest that it may contain substantial proportions of silica [14, 20], or essentially no silica [21]; recent work proposes the composition $\text{SiO}_2 \cdot 6\text{Al}_2\text{O}_3$ for this phase formed from precursors of mullite composition [22].

The results obtained here confirm the above. The polymeric precursor exhibited a sharp exotherm at 1000°C, and the XRD evidence demonstrated that substantial atomic rearrangement of the quasi-amorphous aluminosiloxane material had occurred to produce crystallites of $\gamma\text{-Al}_2\text{O}_3$ and SiO_2 . On the other hand, the coprecipitated material exhibited only a very small exotherm at 1000°C, and in this case, the X-ray and TEM evidence showed that separation of $\gamma\text{-Al}_2\text{O}_3$ and SiO_2 already had occurred at much lower temperatures, perhaps reflecting heterogeneity at the nanometre level in the original coprecipitated hydrous oxides. In this case, the small exothermic event

observed at 1000°C may have been due to the conversion of $\gamma\text{-Al}_2\text{O}_3$ to $\theta\text{-Al}_2\text{O}_3$, or to the decomposition, as above, of small amounts of aluminosiloxane (i.e. atomically homogeneous) material present in the coprecipitate.

The exothermic event near 1200°C can be associated with the formation of mullite as a result of reaction between γ - or $\theta\text{-Al}_2\text{O}_3$ and SiO_2 . This reaction is diffusion-controlled, and therefore sluggish; moreover the free energy at 1200°C is only a few Kilojoules per mole $\text{Al}_6\text{Si}_2\text{O}_{13}$ [23]. Therefore, it is probable that this small exothermic event can be seen in the DTA record only when relatively high heating rates are used.

The XRD results show that the formation of mullite from the coprecipitated powder required higher temperatures, and was much slower than was the case for the polymeric precursor. This probably was due to the sizes of the crystallites of $\gamma\text{-Al}_2\text{O}_3$ and SiO_2 in the two cases. The reaction can take place only at the surfaces of such crystallites. For very small and intimately mixed crystallites such as those which must be formed by decomposition of the polymeric precursor, a small degree of reaction would represent a substantial proportion of the volume of the specimen. Further, it would be expected that the mullite crystallites would be very small, because only a small degree of reaction would be required to consume the reactant particles. This effect was seen in the XRD pattern of polymeric material calcined at 1000°C for 20 min, where the peaks due to mullite were relatively broad. In the case of the coprecipitated material, the crystallites of the reactant oxides were relatively large and well developed, so that longer reaction times and higher temperatures would be required to form mullite in sufficient proportions to be seen by XRD, and the product crystallites would be expected to be relatively large and well formed.

This effect was of no consequence in the studies reported here, because the material was sintered at temperatures near 1600°C to form the final ceramic body, and a desirable microstructure was attained. However, it is clear that some control of the grain size

in the finished material may be achieved by suitable manipulation of the chemical conditions that apply during the formation of the precursor material.

References

1. R. F. DAVIS and J. A. PASK, in "High Temperature Oxides", Part IV, edited by A. M. Alper (Academic Press, New York, 1971) p. 37.
2. W. D. KINGERY, H. K. BOWEN and D. R. UHLMAN, in "Introduction to Ceramics" (Wiley, New York, 1975) p. 583.
3. P. A. LESSING, R. S. GORDON and K. S. MAZDIYASNI, *J. Amer. Ceram. Soc.* **58** (1975) 149.
4. R. ROY, *ibid.* **39** (1956) 145.
5. J. D. CROFTS and W. W. MARSHALL, *Trans. Brit. Ceram. Soc.* **66** (1967) 121.
6. K. S. MAZDIYASNI and L. M. BROWN, *J. Amer. Ceram. Soc.* **55** (1972) 548.
7. D. M. ROY, P. R. NEURGAONKAR, T. P. O. HOLLERAN and R. ROY, *Amer. Ceram. Soc. Bull.* **56** (1977) 1023.
8. T. A. WHEAT, E. M. H. SALLAM and A. C. D. CHAKLADER, *Ceram. Int.* **5** (1979) 42.
9. G. Y. MENG and R. A. HUGGINS, *Mater. Res. Bull.* **18** (1983) 581.
10. M. SUZUKI, S. HIRAISHI, M. TOSHIMURA and S. SÖMIYA, *Yogyo-Kyokai-Shi* **92** (1984) 6.
11. D. W. HOFFMAN, R. ROY and S. KOMARNENI, *J. Amer. Ceram. Soc.* **67** (1984) 468.
12. P. E. DEBELY, E. A. BARRINGER and H. K. BOWEN, *ibid.* **68** (1985) C. 76.
13. S. KANZAKI, H. TABATA, T. KUMASAWA and S. OHTA, *ibid.* **68** (1985) C. 6.
14. A. K. CHAKRABORTY and D. K. GHOSH, *ibid.* **69** (1986) C. 202.
15. J. A. PASK, X. W. ZHANG, A. P. TOMSIA and B. E. YOLDAS, *ibid.* **70** (1987) 704.
16. B. E. YOLDAS, *J. Mater. Sci.* **14** (1979) 1843.
17. F. H. NORTON, *J. Amer. Ceram. Soc.* **22** (1939) 54.
18. R. L. STONE, *ibid.* **35** (1952) 90.
19. B. SONUPARLAK, M. SARIKAYA and I. A. AKSAY, *ibid.* **70** (1987) 837.
20. G. W. BRINDLEY and M. NAKAHIRA, *ibid.* **42** (1959) 319.
21. I. W. M. BROWN, K. J. D. MACKENZIE, M. E. BOWEN and R. H. MEINHOLD, *ibid.* **68** (1985) 298.
22. K. OKADA and N. OTSUKA, *ibid.* **69** (1986) 652.
23. A. C. COOPER, D. A. R. KAY and J. TAYLOR, *Trans. Brit. Ceram. Soc.* **60** (1961) 124.

Received 12 May
and accepted 23 October 1989